

The hydrogenation and direct desulfurization reaction pathway in thiophene hydrodesulfurization over MoS₂ catalysts at realistic conditions: A density functional study

Poul Georg Moses^a, Berit Hinnemann^b, Henrik Topsøe^b, Jens K. Nørskov^{a,*}

^a Center for Atomic-Scale Materials Design (CAMD), Department of Physics, Building 307, Nano DTU, Technical University of Denmark, DK-2800 Kgs. Lyngby, Denmark

^b Haldor Topsøe A/S, Nymøllevej 55, DK-2800 Kgs. Lyngby, Denmark

Received 5 December 2006; revised 20 February 2007; accepted 23 February 2007

Available online 20 April 2007

Abstract

We present density functional theory (DFT) calculations of reaction pathways for both the hydrogenation (HYD) and direct desulfurization (DDS) routes in the hydrodesulfurization (HDS) of thiophene over the different MoS₂ edge structures, which will dominate under typical HDS reaction conditions. Contrary to the generally accepted view, we find that the HYD reaction path, which involves hydrogenation to 2-hydrothiophene followed by hydrogenation to 2,5-dihydrothiophene and subsequent S–C scission, can occur at the equilibrium Mo(10 $\bar{1}$ 0) edge without the creation of coordinatively unsaturated Mo edge sites. This is related to the presence of the metallic-like brim sites also observed in previous STM studies. It is found that the HYD reaction pathway also can occur at the S($\bar{1}$ 010) edge. At this edge, the equilibrium edge structure itself is not active, and sulfur vacancies must be created for the reaction to proceed. It is found that the effective energy barrier for vacancy creation depends on the H₂ partial pressure. The sulfur vacancies at the S($\bar{1}$ 010) edge are also found to be active sites for the DDS pathway. This pathway does involve an initial hydrogenation step to 2-hydrothiophene, followed by S–C scission. Analyzing the relative stabilities of reactants and intermediates suggests that a catalytic cycle may involve elementary steps that start at one type of edge and are completed at the other; for example, many intermediates are more stable at the S edge. The regeneration of the active sites is found to be a crucial step for all of the reaction pathways, and the importance of reactions at Mo brim sites is related to the observation that regeneration is least activated here. It is proposed that an important activity descriptor is the minimum energy required to either add or remove S from the different equilibrium edge structures.

© 2007 Elsevier Inc. All rights reserved.

Keywords: Hydrodesulfurization; Hydrogenation; DFT; Brim Sites; MoS₂; Thiophene; Reaction Mechanism; DDS; HYD

1. Introduction

As the global energy consumption rapidly increases and environmental legislation becomes stricter, the need to upgrade low-quality oil to clean transport fuels increases. To meet current environmental regulations, refiners must remove even the most refractory sulfur-containing species [1–6]. This is generating increased interest in obtaining a detailed description of the catalytic hydrotreating reactions occurring during desulfurization. Hydrodesulfurization (HDS) has been investigated for

many decades, leading to increased insight into the structure of the active catalyst particles, their interactions with the support, the effect of promoters, and the kinetics of the reactions [7]. However, much less is known about the reaction mechanisms and the nature of the active sites, and many different views have been presented [6–12].

Thiophene is a suitable test molecule for studying the HDS reaction because it contains an S atom in a benzene-like ring and also is small. Therefore, thiophene HDS has been the most studied reaction; but there has been considerable debate regarding the mechanism [7,10,13–23]. For instance, it has been difficult to establish to what extent prehydrogenation to dihydrothiophene or tetrahydrothiophene may be necessary before S–C bond cleavage. It also appears that the observed reaction

* Corresponding author.

E-mail address: norskov@fysik.dtu.dk (J.K. Nørskov).

products depend on the reaction conditions [7,22,23]. Tetrahydrothiophene typically is not an intermediate at atmospheric pressure [23], but it may be a major intermediate at high pressure [17] and low temperature [10], because the formation of tetrahydrothiophene is equilibrium-limited at high temperature [10]. A detailed study of the HDS of 2-methylthiophene at high pressure [22] found that the splitting of the S–C bond in tetrahydro-2-methylthiophene (resulting in the formation of a thiol) is faster than the hydrogenation of the thiophene ring or of the pentene to yield pentane. Thus, the hydrogenation activity of the catalyst appears to be an important feature, which can influence the concentration of the reaction products. The proposed thiol intermediate was not observed, leading to the conclusion that the splitting of S–C bonds in thiols is very fast.

For the larger S-containing molecules like dibenzothiophene, it has been established that two parallel routes exist, a direct desulfurization route (DDS) through biphenyl and a hydrogenation route (HYD) in which one of the benzene rings is hydrogenated first [24]. In order to produce the clean transport fuels demanded today, even the very refractory sulfur compounds like 4,6-dimethyldibenzothiophene must be removed [1,2,4,5,7,19,25,26]. For such molecules, the HYD route may become more important than the DDS route, which dominates for unsubstituted dibenzothiophene [4,27]. Despite the established understanding of the pathways and the overall kinetics, little direct insight has been obtained regarding the reaction mechanisms and the surface sites involved in the DDS and HYD pathways. It has even been difficult to reach agreement on the mode of adsorption of the reactants. For instance, thiophene has been found to either exclusively adsorb in a so-called η_1 mode (e.g., standing up and binding only through S [28,29]) or adsorb primarily in a so-called η_5 mode (e.g., lying down, bonded through S and the four C atoms), with only a small fraction of the molecules being present in the η_1 mode [30].

Insight into the mechanism of HDS also has been obtained from numerous studies on activity correlations [7,31,32], which have been taken as evidence for MoS₂ edge vacancies being the active sites in HDS, because vacancy formation generally has been assumed to take place at the MoS₂ edges. In support of this, basal plane surfaces have been observed to be inactive [33]. For hydrogenation reactions, the activity also has been observed to correlate with the number of MoS₂ or WS₂ edges sites [34,35], and vacancies have been concluded to be the active sites for such reactions. However, in general it is difficult to draw firm conclusions from such activity correlations [7], because a variety of other species, like SH groups [36], also may be located at the edges. Further support for the importance of vacancies has been provided from experimental studies of the effect of prereduction temperature [37,38]. Moreover, the observed activity correlation with the metal–sulfur bond strength, leading to the formulation of the bond energy model (BEM), suggest that vacancy formation is a key aspect of HDS [39].

Because both HDS and hydrogenation activities have been observed to correlate with the number of MoS₂ (WS₂) edge sites, some authors have suggested [40,41] that the sites for the DDS route and the HYD route are similar. Indeed, kinetic models based on this proposal can provide a good fit of ki-

netic results. However, a number of effects strongly suggest that DDS and hydrogenation sites are not the same. For example, the presence of methyl groups in dibenzothiophene may severely reduce the activity for S removal via DDS without significantly affecting the hydrogenation activity [4]. In addition, H₂S is a strong inhibitor for S removal via DDS but has only a minor effect on hydrogenation [27]. Evidence for different sites for HYD and DDS also comes from studies of the effect of nitrogen compounds [7,26,42–52]. In contrast to the effect of H₂S, the presence of basic nitrogen compounds is observed to mainly inhibit the HYD route with only a moderate effect on DDS. The inhibiting effect was found to correlate with the proton affinity of the nitrogen compounds [44,45]; this result also suggests that different sites are involved in HYD and DDS. Based on the observation that quite large molecules may be desulfurized via the HYD route, Ma and Schobert [53] suggested that the hydrogenation sites are multiple vacancy sites on the Mo(10 $\bar{1}$ 0) edges capable of π -bonding the large molecules. The presence of such sites has been discussed in the literature [7], because the single-bonded sulfur atoms created by simply cleaving the bulk structures at the Mo(10 $\bar{1}$ 0) edges were proposed to be unstable.

Recently, it has become possible to use density functional theory (DFT) methods to address a number of issues relevant for HDS [54–72]. In the first DFT study of MoS₂ and Co-MoS structures, Byskov et al. [71] found that it is energetically very unfavorable to create the “naked” Mo edges, where Mo is exposed at the edge and only 4-fold coordinated, and they concluded that such structures probably are not present under realistic HDS conditions [71]. Subsequent DFT studies have supported this conclusion [56,67,70]. Even though multiple vacancy sites may be very reactive [59,62,64], they are expected to readily react with H₂S, and reactions involving such sites should be extremely strongly inhibited by H₂S. Because the hydrogenation reactions are not poisoned by H₂S, these results show that some other sites must be involved in HYD. The first study of mechanistic aspects of HDS using DFT was carried out by Neurock and Van Santen, who studied the HDS of thiophene over Ni_xS_y clusters [65]. Although the study does not directly relate to MoS₂ catalysts, coordinatively unsaturated Ni sites were found to be very reactive.

Recently, it has been possible to obtain important clues regarding the hydrogenation sites and the HYD pathway from scanning tunneling microscopy (STM) studies [61]. Such studies have provided atom resolved images of the MoS₂ nanostructures; when they are combined with DFT calculations, quite detailed information may be obtained from the images [56, 57,61,73,74]. These combined studies clearly show that naked Mo(10 $\bar{1}$ 0) edges are not present at ultrahigh vacuum conditions. In contrast, the results show in agreement with the DFT calculations [54,56,63,69,71] that the Mo atoms will tend to maintain the full sulfur coordination of 6. This is achieved by extensive edge reconstruction. Quite surprisingly, it was found that these fully sulfur-saturated Mo(10 $\bar{1}$ 0) edges of MoS₂ have some sites with metallic character [56,73,75]. These so-called “brim” sites could bind thiophene and were observed to be involved in further hydrogenation reactions [61]. One S–C bond in thiophene appeared to be cleaved at the brim site, and the resulting ad-

sorbed butenethiolate could be observed [61]. This is interesting, because such thiolates or thiols have been proposed to be key intermediates in many of the HDS mechanisms proposed in the literature [7,22]. However, at realistic HDS conditions, this intermediate has not yet been detected, presumably due to its high reactivity. In the STM study [61], the completion of the HDS reaction could not be observed. Because the MoS₂ clusters only exposed the Mo(10 $\bar{1}$ 0) edge, this study [61] did not yield any information about the possible role of S($\bar{1}$ 010) edges. Also note that the structures observed in the STM experiments might not be those structures, which are stable under reaction conditions [61].

The structures and intermediates present under reaction conditions generally are not accessible for study by direct imaging methods, but they can be studied by DFT calculations. Indeed, it has been found experimentally [57] and theoretically [54,56,63,69,70] that the MoS₂ edge structures may be very labile, and quite different structures may exist depending on the reaction conditions. In the real HDS catalyst, the MoS₂ and WS₂ structures also may expose the S($\bar{1}$ 010) edges [57,76]. A key objective of the present study is to examine reactions at the S($\bar{1}$ 010) edges, which are predicted to be present at reaction conditions.

The present study used DFT to investigate HDS of thiophene. The calculational details are described in Section 2. An important problem with most reaction pathway studies has been that the assumed structures may be very different from those actually present at HDS conditions. Therefore, a key goal of the present study is to perform calculations on the type of structures that will be present during HDS catalysis. Section 3.1 discusses the relevant structures and edge configurations to lay the groundwork for studying the reaction pathway. The energetically most stable structures for both the Mo(10 $\bar{1}$ 0) edge and the S($\bar{1}$ 010) edge under typical reaction conditions are described. Sections 3.2–3.4 discuss the results on hydrogenation, S–C cleavage and site regeneration reactions at those edges. These detailed results are subsequently used to discuss some more general themes. The influence of reaction conditions is found to be quite significant, and these aspects are discussed in Section 3.5. Sections 3.6 and 3.7 present an analysis of the hydrogenation and S–C bond scission reactions and interplay between the two different edge sites in those reactions based on the determined reaction paths and the availability of the active sites. Section 3.8 discusses the relative role of different elementary reactions and pathways during HDS of thiophene. To avoid excessive repetition and to aid the presentation of the results, we have summarized many of the detailed results regarding the reaction pathways, the stabilities of the intermediates, and key activation energies in Figs. 3–7 and Table 1. Detailed comments regarding each elementary step and the nature of the intermediates are given in the following sections, and further details are provided in supplementary information.

2. Calculational details

An infinite stripe model, which previously has been proven successful to investigate MoS₂-based systems [55,56,77,78],

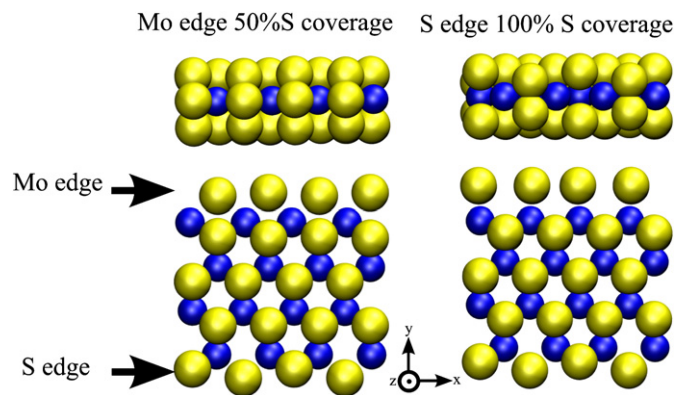


Fig. 1. The 4×4 supercells used for studies of the Mo edge with 50% S coverage and the S edge with 100% S coverage. Color code: sulfur (yellow), molybdenum (blue). (For interpretation of the references to color in this figure legend, the reader is referred to the web version of this article.)

is used to investigate the edges of MoS₂ and is depicted in Fig. 1. The infinite stripe exposes both the Mo edge and the S edge. The supercell has 4 Mo atoms in the x -direction and 4 Mo atoms in the y -direction, to allow for important reconstructions with a period of 2 in the x -direction and to allow decoupling of the Mo edge and the S edge in the y -direction. The stripes are separated by 14.8 Å in the z -direction and 9 Å in the y -direction. This model represents MoS₂ structures with no support interactions such structures are similar to the type II structures found in today's high-activity commercial catalysts [78].

The plane wave density functional theory code DACAPO [79,80] was used to perform the DFT calculations. The Brillouin zone was sampled using a Monkhorst–Pack k -point set [81] containing 4 k -points in the x -direction and 1 k -point in the y - and z -directions. The calculated equilibrium lattice constant of $a = 3.215$ Å and compares well to the experimental lattice constant of 3.16 Å [82]. A plane-wave cutoff of 30 Rydberg and a density wave cutoff of 45 Rydberg were used using the double-grid technique [83]. Ultrasoft pseudopotentials are used except for sulfur, where a soft pseudopotential was used [84,85]. A Fermi temperature of $k_B T = 0.1$ eV was used for all calculations, and energies were extrapolated to zero electronic temperature. The exchange correlation functional PW91 [86] was used. The convergence criterion for the atomic relaxation is that the norm of the total force should be <0.15 eV/Å, which corresponds approximately to a max force on one atom <0.05 eV/Å. The nudged elastic band (NEB) method was used to find energy barriers [87], together with the adaptive nudged elastic band approach [88] and cubic spline fits to the energy and the forces. Figures of atomic structures were created using VMD [89].

Unless notes otherwise, all adsorption energies were calculated using the equation

$$\Delta E_{\text{ad}} = E_{\text{molecule/MoS}_2} - E_{\text{MoS}_2} - E_{\text{molecule(g)}},$$

where $E_{\text{molecule/MoS}_2}$ is the energy of the system with the molecule bound to the surface, E_{MoS_2} is the energy of the stripe, and $E_{\text{molecule(g)}}$ is the energy of the molecule in vacuum. Molecules in vacuum were calculated using the same setup as for

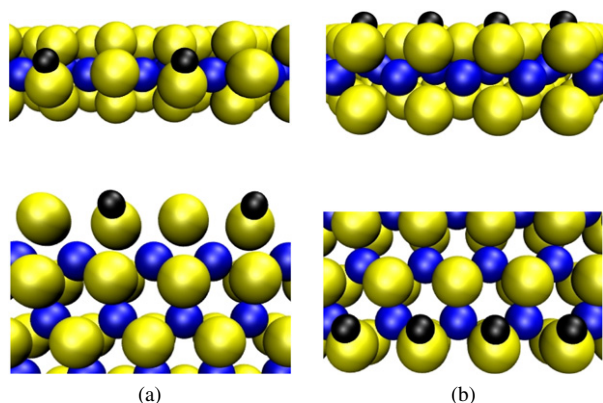


Fig. 2. The equilibrium edge configurations at HDS conditions ($P_{\text{H}_2} = 10$ bar, $P_{\text{H}_2}/P_{\text{H}_2\text{S}} = 100$, and $T = 650$ K). (a) The Mo edge with 50% S coverage and 50% H coverage. (b) The S edge with 100% S coverage and 100% H coverage.

stripe calculations but using a supercell, which ensures at least 11 \AA vacuum between neighboring molecules, using a Fermi temperature of $k_{\text{B}}T = 0.01$ eV, using only the gamma point in the Brillouin zone sampling. For all structural relaxations, the convergence criterion is that the norm of the total force should be <0.05 eV/ \AA .

3. Results and discussion

3.1. The choice of active surfaces and elementary reactions

The starting point of this investigation of HDS of thiophene is the recently improved understanding of the edge configurations at HDS conditions, which has been provided by several DFT studies [54,56,63,69,70]. As a starting point, we use the phase diagrams developed previously [56], which describe the edge structures as function of the chemical potential of S and H. The equilibrium edge configuration at HDS conditions (e.g., $P_{\text{H}_2} = 10$ bar, $P_{\text{H}_2}/P_{\text{H}_2\text{S}} = 100$ and $T = 650$ K, which are used throughout the article as an example of HDS conditions) determined in previous work [56] was recalculated with the calculational setup described in Section 2. We find essentially the same structures and adsorption energies as reported previously [56]; these equilibrium edge structures are shown in Fig. 2. HDS conditions vary depending on the crude oil being treated; the hydrogen pressure may vary from 10 to 200 bar, and $P_{\text{H}_2}/P_{\text{H}_2\text{S}}$ also may vary depending on the reactor setup. The structure presented in Fig. 2 is the most stable structure over most of this range, with the exception that there may be more H atoms present at the S edge at high hydrogen pressures. S and H adsorption at sites at the edges of MoS_2 introduces structural changes; therefore, the definition of coverage of S and H needs to be refined; in this paper, we define the S coverage as the percentage of S present at the edge, with 100% being the S coverage of the fully sulfided edge (i.e., completely covered by S dimers). Using this definition, the S coverage is 50% at the Mo edge and 100% at the S edge (Fig. 2). Furthermore, we define the H coverage as the fraction of H atoms present per edge unit cell in the 4×4 structure; for example, 4 H atoms correspond to 100% H coverage. Using this definition, the H coverage in Fig. 2 is 50% at the Mo edge and 100% at the S edge. This defi-

inition allows for coverage above 100%, when more than four H atoms are present per unit cell. It should be emphasized that the structure for each “coverage” represents a new unique structure, and thus “coverage” should not be understood in the traditional sense, where it is the coverage of identical sites.

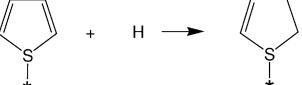
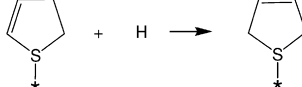
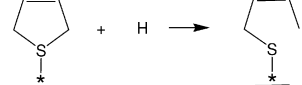
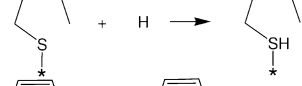
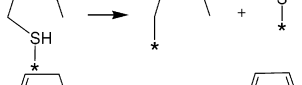

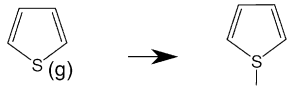

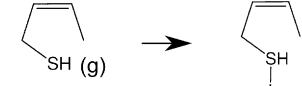
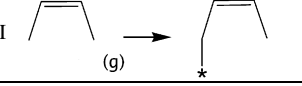
In the literature, “naked” $\text{Mo}(10\bar{1}0)$ edges with a coverage of 0% S have been considered as possible sites for hydrogenation reactions [53]. In this configuration, the $\text{Mo}(10\bar{1}0)$ edge contains Mo atoms coordinated to only four sulfur atoms, compared with a coordination number of 6 in the bulk. This situation is energetically very unfavourable under HDS conditions. In contrast, we find [56] an equilibrium S coverage of 50% at the Mo edge under HDS conditions. Note that in Fig. 2, the Mo coordination number is 6 at both edges. The H coverage at the S and Mo edges given in Fig. 2 corresponds to $P_{\text{H}_2} = 10$ bar. However, we show that it is possible to further increase the H coverage at the S edge by increasing the H_2 pressure, resulting in a H coverage above 100% (see atomic configuration 2 in Fig. 4). Such an increase is not possible at the Mo edge due to strong interaction between H atoms, as discussed further in Section 3.5 and also reported previously [78]. Our calculations show that a basic requirement for the removal of S from thiophene and other S-containing compounds is an available site for the adsorption of removed S. In this connection, an interesting finding is that the equilibrium edge configuration at the Mo edge allows for the addition of an S atom, whereas the equilibrium configuration at the S edge is fully covered by S and H atoms and does not allow for such an addition. Therefore, at the S edge, a vacancy must be created before S removal at the S edge.

Experimental studies of thiophene HDS have suggested that various pathways may be involved, and that the relative involvement of these pathways depends on the reaction conditions [7,10]. The elementary reactions in the different proposed reaction pathways include both hydrogenation and S–C bond scission reactions; thus, we have chosen to investigate both elementary hydrogenation and S–C bond scission reaction steps. Many different steps have been considered; to simplify the subsequent discussion, we summarize the elementary reactions investigated in the present study in Table 1, together with the calculated reaction and activation energies. The choice of elementary reactions and intermediates has been guided by recent STM and DFT studies, which have shown that thiophene hydrogenation and S–C scission can occur at the fully sulfided Mo edge [61]. Except for 2-hydrothiophene, all of the other intermediates given in Table 1 have been reported to be present during HDS of thiophene [7,90,91]. The reason that 2-hydrothiophene has not been observed experimentally is most likely related to the fact that it is not a stable molecule in the gas phase. Furthermore, the present study shows that the subsequent hydrogenation of 2-hydrothiophene to 2,5-dihydrothiophene is a nonactivated process.

We investigate both the HYD and DDS pathway of thiophene HDS. We define the difference between the DDS and the HYD pathway so that it is the DDS pathway when the initial S–C cleavage (reaction VI in Table 1) occurs in 2-hydrothiophene after the first hydrogenation step (reaction I in Ta-

Table 1

An overview of the reactions involved in HDS of thiophene including the activation barriers (E_a) and energy change (ΔE) of the reactions

| Reaction | S edge | | Mo edge | |
|--|--|--|-------------------|--------------------|
| | E_a (eV) | ΔE (eV) | E_a (eV) | ΔE (eV) |
| I  | 0.80 | 0.43 | 0.57 | 0.57 |
| II  | 0.00 | -1.02 | 0.00 | -0.74 |
| III  | 0.82 | -0.78 | 1.13 | 0.51 |
| IV  | 1.63 | 1.09 | 0.14 | -0.26 |
| V  | 0.00 | -0.66 | 0.12 | -0.41 |
| VI  | 0.21 | -1.11 | 1.10 | 1.09 |
| VII $2\text{HS-}^* \rightarrow \text{H}_2\text{S-}^* + \text{S-}^*$ | 1.70 ^a 1.49 ^b | 1.57 ^a 1.32 ^b | 1.00 ^c | 0.7 ^c |
| VIII $(1/2)\text{H}_2(\text{g}) + ^* \rightarrow \text{H-}^*$ | | -0.57 ^a -0.11 ^b | | -0.33 ^d |
| IX $\text{H}_2\text{S}(\text{g}) + ^* \rightarrow \text{H}_2\text{S-}^*$ | | -0.12 ^h | | -0.19 ^e |
| X  | | 0.21 ^g | | -0.07 ^f |
| XI  | | -0.59 ^g | | -0.12 ^f |
| XII  | | -0.52 ^g | | -0.12 ^d |
| XIII  | | -0.05 ⁱ | | -0.28 ^d |

^a Low H_2 pressures.^b High H_2 pressures.^c Calculated as $E_{\text{VII}} = \Delta E_1 + E_2$, where ΔE_1 is the energy change of reaction 1: 2H-S (50% H coverage 50% S) + S (0% H and 62.5% S) + S-S (0% H and 62.5% S) \rightarrow S (25% H coverage 50% S) + HS (50% H and 62.5% S) + H-S-S (50% H and 62.5% S) and E_2 is the activation energy of reaction 2: HS (50% H and 62.5% S) + H-S-S (50% H and 62.5% S) \rightarrow $\text{H}_2\text{S-S}$ (Mo edge 50% S).^d Adsorption at the Mo edge with 50% S and 25% H.^e Adsorption at the Mo edge with 50% S and 0% H.^f Adsorption at the Mo edge with 50% S and 50% H.^g Adsorption at the S edge with 87% S and 75% H.^h Adsorption at the S edge with 87% S and 50% H.ⁱ Adsorption at the S edge with 100% S and 25% H.

ble 1) and the HYD pathway when S–C cleavage (reaction III in Table 1) occurs in 2,5-dihydrothiophene, which is formed by two successive hydrogenation steps (reactions I and II in Table 1). It is interesting to note that the thiophene DDS and HYD pathways involve a common prehydrogenation step, because a similar common prehydrogenation step has been proposed in the HYD and DDS pathway for DBT and 4,6-DMDBT [41].

In what follows, we summarize the reactions in the HYD pathway as we have investigated them at both the Mo and S edges. The HYD pathway involves reactions I–V and reactions VII–XIII in Table 1. The reactions occur in the following order: X–I–II–III–IV–V–VII–IX. Reaction I in Table 1 hydrogenates thiophene and forms 2-hydrothiophene, which is then further hydrogenated (reaction II) to produce 2,5-dihydrothiophene.

The removal of S from 2,5-dihydrothiophene proceeds via initial S–C bond scission (reaction III) with *cis*-2-butenethiolate as a product, followed by *cis*-2-butenethiol formation by a H transfer reaction (reaction IV). Then *cis*-2-butene is the product formed by the final S–C scission (reaction V). In this context, it should be noted that the present study also investigates the S extrusion from *cis*-2-butenethiol, because it is an intermediate in the HYD pathway. It is quite likely that *cis*-2-butene will react further either by hydrogenation to butane or by intramolecular rotation to form *trans*-2-butene. We do not consider these here because they occur after S removal and are not important for sulfur removal. Further hydrogenation of 2,5-dihydrothiophene to tetrahydrothiophene has not been investigated, because we have assumed that tetrahydrothiophene is a likely intermediate only at high H₂ and low temperatures, because the presence of tetrahydrothiophene has been shown to be equilibrium-limited at temperatures typical for HDS conditions [10].

The DDS of thiophene was investigated using the following reaction path: reactions X–I–VI–(IV–V) in Table 1. The DDS pathway was initiated by thiophene adsorption (reaction X), followed by the hydrogenation of thiophene (reaction I), forming 2-hydrothiophene. Then the initial S–C bond was broken (reaction VI) and *cis*-butadienethiolate was formed. The further removal of S from *cis*-butadienethiolate was not investigated directly; however, these reactions are assumed to be very similar to reactions IV and V, because the involvement of the carbon chain is insignificant in these reactions, which are dominated by H diffusion and addition. The product of the DDS pathway is *cis*-butadiene under the assumption that the final S–C bond scission reaction is similar to reactions IV and V. *Cis*-butadiene may react further by hydrogenation or intramolecular rotation.

The reaction pathways shown in Figs. 3–6 have been constructed under the assumption that H₂ in the gas phase is in equilibrium with the H atoms adsorbed at the edge of MoS₂. This assumption is justified by the fact that experimentally H₂ dissociation is not found to be the rate-determining step [7,10]. Previous DFT studies have found the barrier to be 0.9–1 eV at the Mo edge with 50% S coverage [72,92]; however, these studies used a unit cell, which resulted in a H coverage after dissociation equal to 66 or 100%, respectively. The H adsorption energy at the Mo edge is highly dependent on the H coverage [78], and it can be speculated that the barrier changes when the H coverage is lowered to 50%, corresponding to HDS conditions. There have been no studies of the H₂ dissociation at the S edge of MoS₂; the only similar result is for the S edge promoted with 50% Co and with S coverage of 75%, where the barrier was found to be 0.6 eV [68]. The DFT results indicate that at certain reaction conditions (e.g., low hydrogen pressures), there could be an influence on the apparent activation energy due to H₂ dissociation; however, in the present study we have assumed that this is not the case at HDS conditions, and thus the hydrogen addition steps are not included in the reaction pathways. (A complete reaction path in which H addition steps are included is provided in supplementary information.) Furthermore, we contracted the hydrogenation of

thiophene reactions (reactions I and II) to one barrier, because we found that only reaction I was activated.

3.2. The HYD pathway at the Mo edge

Using the elementary steps discussed in Section 3.1, we determined the detailed potential energy diagram for the HYD reaction pathway at the Mo edge; the results are depicted in Fig. 3. To arrive at the diagram shown in Fig. 3, we investigated the intermediates in various configurations as part of determining the minimum energy and the optimal reaction pathway. We evaluated the adsorption of the cyclic intermediates both above edge S atoms and in bridge positions between edge S atoms. Furthermore, we investigated both the η_1 (binding through the S atom) adsorption mode and the η_5 (binding through the π system) adsorption mode. For thiophene, we considered both adsorption modes proposed in the literature based on IR or INS studies [28–30,93] or proposed based on analogous structures observed in organometallic complexes [94]. We find that the preferred adsorption site for 2,5-dihydrothiophene is in between the front row S atoms, which is the location of the brim at the Mo edge at HDS conditions [56]; thus, there is no direct binding to the Mo atoms. Thiophene η_1 and η_5 adsorption at both the brim site and on top of edge S atoms are very similar in energy (within 0.02 eV); therefore, all of these adsorption modes will be expected to be present at HDS conditions. The present results thus support the conclusion from the INS experiments where both the η_1 and η_5 adsorption modes were observed [30]. However, the possibility that van der Waals (vdW) forces will stabilize one of the adsorption configurations cannot be ruled out. Such forces are not included in present-day exchange correlation functionals, and thus we cannot assess the importance of vdW forces. It should be emphasized that the present study investigates the adsorption at the equilibrium edge configurations under HDS conditions (50% H coverage, 50% S coverage). Clearly, the adsorption modes will change when the experimental conditions are changed and new edge structures are created. For example, a recent theoretical investigation found that the η_1 mode was most stable at a reduced Mo edge with a vacancy [95], but such very reduced Mo edges most likely will be present only in insignificant numbers under HDS conditions.

The HYD pathway at the Mo edge (Fig. 3) is initiated by thiophene adsorption at the brim site (reaction X). Following this, two hydrogenation reactions occur (reactions I and II in Table 1), resulting in the formation of 2,5-dihydrothiophene. Furthermore, the overall barrier of the hydrogenation steps is given by the barrier of reaction I, because reaction II is non-activated. Thus, the reaction product (2-hydrothiophene) of reaction I is not expected to be abundant. This may explain why 2-hydrothiophene has never been observed. The hydrogenation reactions involve H from SH groups, which are present at the Mo edge. The binding energy of H at the 50% S-covered Mo edge depends on the H coverage, as also reported previously [78]; therefore, it will primarily be the H atoms corresponding to 50%, which will participate because H is too strongly bound (–0.7 eV) at lower coverage. H adsorption at coverage >50%

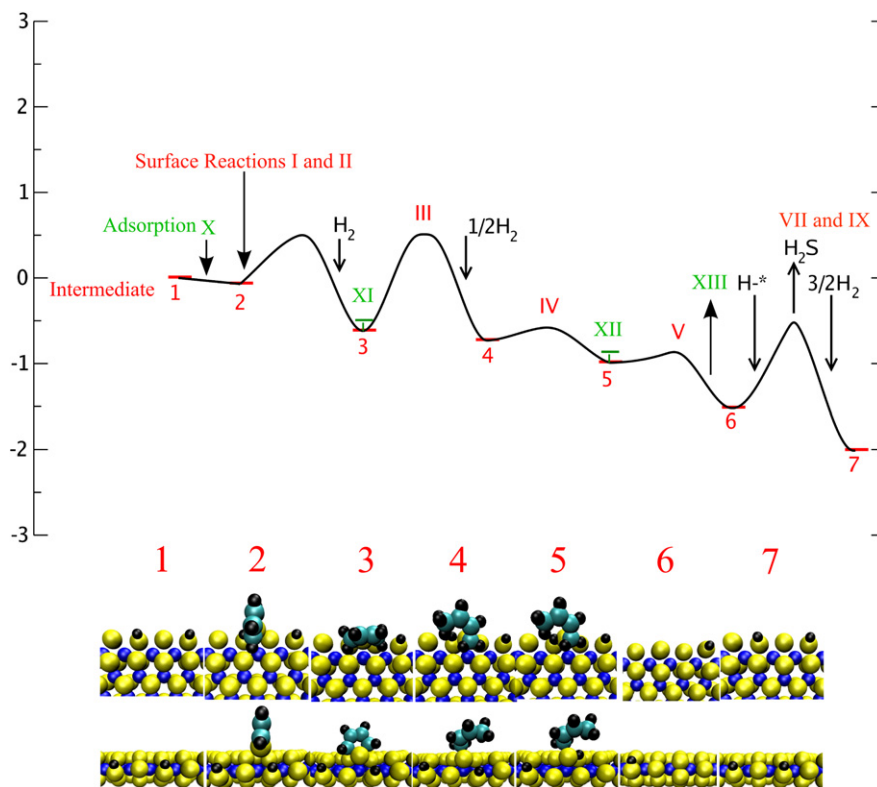


Fig. 3. The Mo-edge thiophene HYD pathway. The reference energy is the equilibrium edge configuration under HDS conditions (Mo edge with 50% S and 50% H) and thiophene in the gas phase. The atoms have the following color scheme: yellow, sulfur; blue, molybdenum; cyan, carbon; black, hydrogen. Arabic numerals denote intermediates, and Roman numerals denote reactions. (For interpretation of the references to color in this figure legend, the reader is referred to the web version of this article.)

has an endothermic binding energy (0.4 eV) [78] and are not occupied.

The initial hydrogenation steps are followed by reaction III, which breaks the first S–C bond in 2,5-dihydrothiophene and forms *cis*-2-butenethiolate. *Cis*-2-butenethiol is formed by H transfer in reaction IV, and finally S is removed by breaking the last S–C bond in the thiol in reaction V. Note that the removal of S from *cis*-2-butenethiol (reaction V) has a very low barrier (0.1 eV) and that the most difficult step is the initial S–C bond breaking. Removal of S from the thiol leaves behind an S atom. Subsequently, the active site must be regenerated to complete the catalytic cycle. The activation energy of regenerating the active site (reaction VII) is similar to the activation energy of the cleavage of the first S–C bond (reaction III).

STM experiments did not reveal the removal of S from thiolate [61]. This is not in contradiction with the present findings, because the equilibrium edge structure under the STM experimental conditions differs from that under reaction conditions. Under the STM conditions, the edges are completely covered with sulfur dimers (100% sulfur coverage). This surface does not allow the accommodation of an extra S atom, and thus the reaction stops once thiolate is formed. The present results show that it is of key importance that H atoms are present at the Mo edge at HDS conditions and that these H atoms react readily with thiophene and the intermediates. Thus, the Mo edge configuration present at HDS conditions is more suitable for HDS reactions than the highly sulfided Mo edge present at STM

experimental conditions. The relative importance of the different hydrogenation reactions, the S–C bond scission reactions, and regeneration of the active site are explored further in Sections 3.5–3.8.

3.3. HYD pathway at the S edge

In the preceding section, we dealt with the HYD reaction pathway at the Mo edge. Under realistic HDS conditions, MoS₂ is likely to expose S edges as well, and possible reactions at this edge must also be considered [54,57]. The calculated potential energy diagram of the HYD reaction path at the S edge is shown in Fig. 4. It consists of reactions I–V and reactions VII–XIII in Table 1.

The HYD reaction pathway is initiated by vacancy formation (reaction VII), because a vacancy is needed to bind the intermediates and for the final removal of S from the organic molecule. We calculated the barriers for creating vacancies at high and low hydrogen pressures corresponding to 125% H and 100% H coverage, respectively; see Fig. 4. The binding energy of H decreases when there is more than one H atom per S dimer at the edge, as seen in Table 1. The importance of such weakly bound and more reactive H atoms is discussed further in Section 3.5, which also includes a discussion of the influence of the hydrogen pressure on the equilibrium H coverage.

After vacancy creation, the HYD pathway continues with adsorption of thiophene (reaction X) at the vacancy (corre-

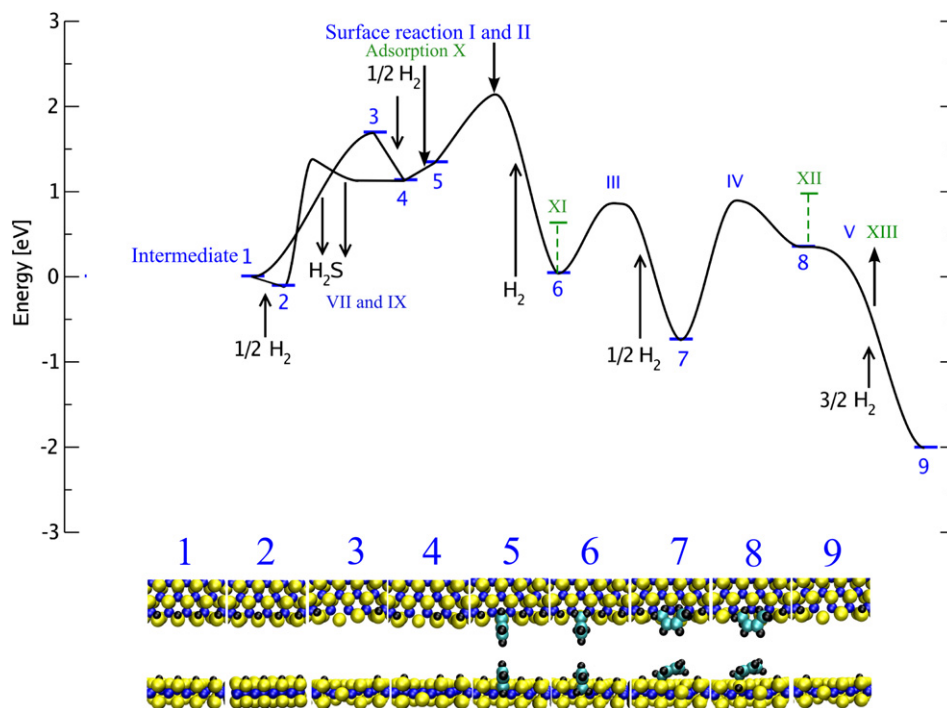


Fig. 4. The S-edge thiophene HYD pathway. The reference energy is the equilibrium edge configuration under HDS conditions (S edge with 100% S and 100% H) and thiophene in the gas phase. The color scheme for the atoms is the same as in Fig. 1. Arabic numerals denote intermediates, and Roman numerals denote reactions. (For interpretation of the references to color in this figure legend, the reader is referred to the web version of this article.)

sponding to 75% S coverage and 75% H coverage); this is endothermic (0.2 eV at 75% H coverage and 0.0 eV at 50% H coverage). The present adsorption mode is an end-on η_1 adsorption through the sulfur atom. Thus, thiophene adsorption will occur only if the van der Waals forces (which are not included in the present exchange correlation functional) are strong enough to give an exothermic adsorption energy; otherwise, thiophene hydrogenation and adsorption may occur in a concerted manner. Thus we expect that thiophene will be observed in high concentration only at the S edge in η_1 adsorption mode at low temperatures or at edges far from HDS equilibrium edge configurations with vacancies and low H coverage. This is in agreement with a recent theoretical study of thiophene adsorption at the S edge of stacked MoS₂ that found it to be strongest at the S edge with multiple vacancies or 0% H coverage [95]. The thiophene coverage at the vacancy sites is expected to be very small at HDS conditions, due to the endothermic adsorption energy (0.2 eV). The first hydrogenation reaction (reaction I), resulting in the formation of 2-hydrothiophene, had a higher barrier than the same reaction at the Mo edge (0.8 eV vs 0.6 eV), and the second hydrogenation reaction was also nonactivated at the S edge vacancy. The higher reaction barrier of the first hydrogenation step is ascribed to the stronger binding energy of H at the S edge. In fact, the results show that the SH bond strength is a key parameter for all the hydrogenation reactions including the reaction involved in site regeneration. The hydrogenation reactions are followed by reactions III, IV, and V, where the two S–C bond scission reactions (reactions III and V) have lower barriers than at the Mo edge, whereas the creation of *cis*-2-butenethiol has a higher barrier (reaction IV). The highest barrier involved

in the HYD pathway is the initial vacancy and the H₂S formation step.

We investigated to what extent it could be possible that adsorption and hydrogenation could occur without the presence of an S vacancy at the S edge. For this purpose, we evaluated the S edge with 100% S and 75% H, which is a slightly lower H coverage than the equilibrium edge configuration (100% H), to leave room for thiophene adsorption. Thiophene adsorption at the S edge with 100% S and 75% H is in fact slightly exothermic (−0.1 eV). But this adsorption energy is smaller than the H adsorption energy (−0.6 eV) at the same site. Thus, H atoms will adsorb predominately at these sites and create the equilibrium structure, and the adsorption of thiophene is favored only at reaction conditions, where hydrogen pressure is low and thiophene pressure is high. Nevertheless, a full microkinetic model must be developed before the catalytic role of the “nonvacancy” sites can be evaluated in detail.

The relative catalytic importance of the hydrogenation reactions, S–C bond scission reactions, and regeneration of the active site at the S and Mo edge are further discussed in Sections 3.5–3.8.

3.4. DDS pathway at the Mo and S edges

As discussed in Section 3.1, the DDS pathway is characterized by the initial S–C scission reaction occurring immediately after the formation of 2-hydrothiophene. Thus, the first step after adsorption of thiophene (reaction X) is hydrogenation to 2-hydrothiophene (reaction I), followed by S–C bond scission (reaction VI) to *cis*-butadienethiolate. The final S removal from *cis*-2-butadienethiolate is assumed to be similar to the final S

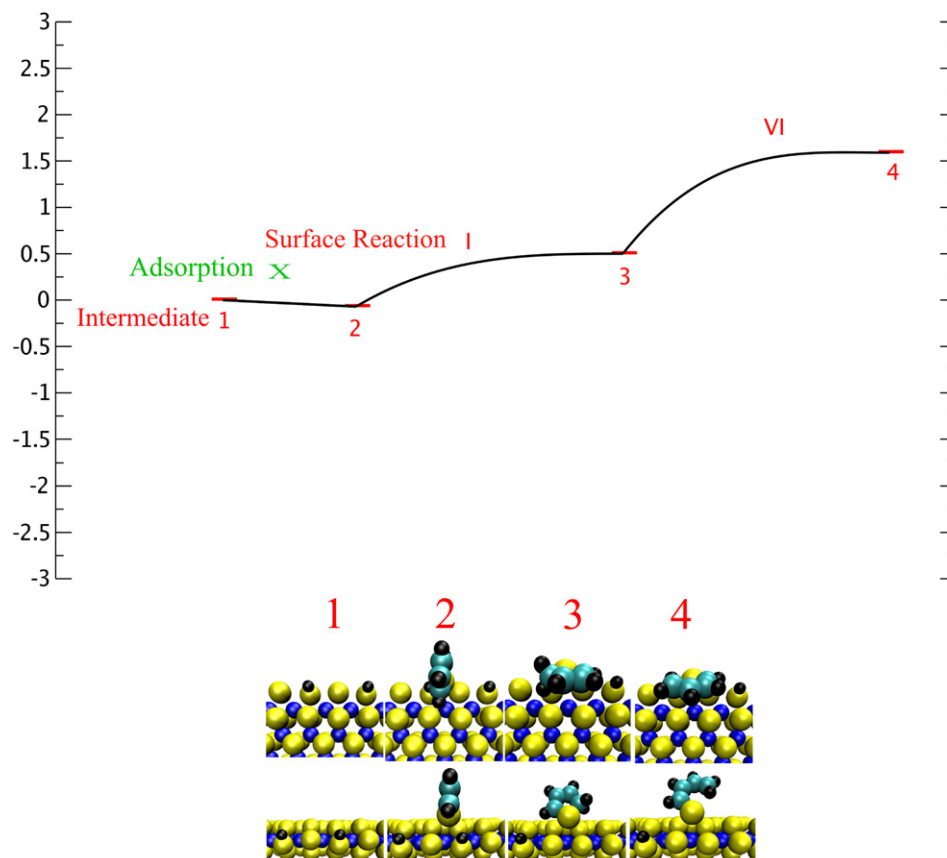


Fig. 5. The Mo-edge DDS pathway of thiophene. The reference energy is the equilibrium edge configuration at HDS conditions (Mo edge with 50% S and 50% H) and thiophene in the gas phase. The color scheme for the atoms is the same as in Fig. 1. Arabic numerals denote intermediates, and Roman numerals denote reactions. (For interpretation of the references to color in this figure legend, the reader is referred to the web version of this article.)

removal from *cis*-2-butenethiolate. The calculated potential energy diagrams of the DDS pathway at the Mo edge and the S edge are shown in Figs. 5 and 6, respectively. At the equilibrium Mo edge (50% S coverage and 50% H coverage), the DDS pathway is initiated by hydrogenation (reaction I), followed by S–C bond scission (reaction VI). The DDS pathway at the equilibrium S edge (100% S coverage and 100% H coverage) must (as discussed in Section 3.3) be initiated by vacancy formation (reaction VII). This is then followed by adsorption of thiophene (reaction X), the initial hydrogenation step (reaction I), and S–C bond scission (reaction VI). The barrier of reaction VI is 0.2 eV at the S edge, which is 0.9 eV lower than the barrier at the Mo edge. The present results indicate that the S edge vacancy site has a higher activity in elimination reactions of S–C bonds, which could indicate that the S edge vacancy site more readily eliminates the S–C bond in the DDS of DBT and similar molecules. The availability of the active site and the relative importance of the S and Mo edge in DDS are discussed in Sections 3.1 and 3.7.

3.5. The influence of hydrogen and H₂S pressure on the availability of the active sites

The brim site at the Mo edge and the vacancy site at the S edge are fundamentally different, and the interplay between the sites will depend on the relative availabilities of the sites. The

Mo edge brim site is present at the equilibrium edge configuration, which has 50% S coverage and 50% H coverage, and the site is located in between the front-row S atoms with a neighboring H atom. In contrast to the readily available brim site, a large concentration of vacancy sites is not present at the S edge. Table 1 and Fig. 4 show that the energy required to remove S from the S edge by creating H₂S depends on the H₂ pressure, in the sense that at high H₂ pressures, the coverage of weakly bound H atoms becomes quite large, and this H gives a lower barrier for vacancy formation than the more strongly bound H. At low H₂ pressure, and thus at low coverage of weakly bound H atoms, the overall barrier of H₂S formation is given by the lowest of $E_{\text{overall}} = E_{\text{a}}^{\text{strong}}$ and $E_{\text{overall}} = E_{\text{a}}^{\text{weak}} + \Delta E$, where $E_{\text{a}}^{\text{weak}}$ is the activation energy of H₂S formation involving the weakly bound H atoms, $E_{\text{a}}^{\text{strong}}$ is the activation energy of H₂S formation involving the strongly bound H atoms, and ΔE is the energy difference in binding energy between the weakly and strongly bound H atoms. At high H₂ pressure, and thus at high coverage of the weakly bound H atoms, the overall energy barrier is given by $E_{\text{overall}} = E_{\text{a}}^{\text{weak}}$. In the current work, high coverage is defined as 0.8, which corresponds to approximately 80 bar hydrogen pressure. Quantification of high coverage could be possible using a microkinetic model. The H binding energy is -0.6 eV when only a single H is bound to each S dimer, whereas an additional H added to an S dimer has a binding en-

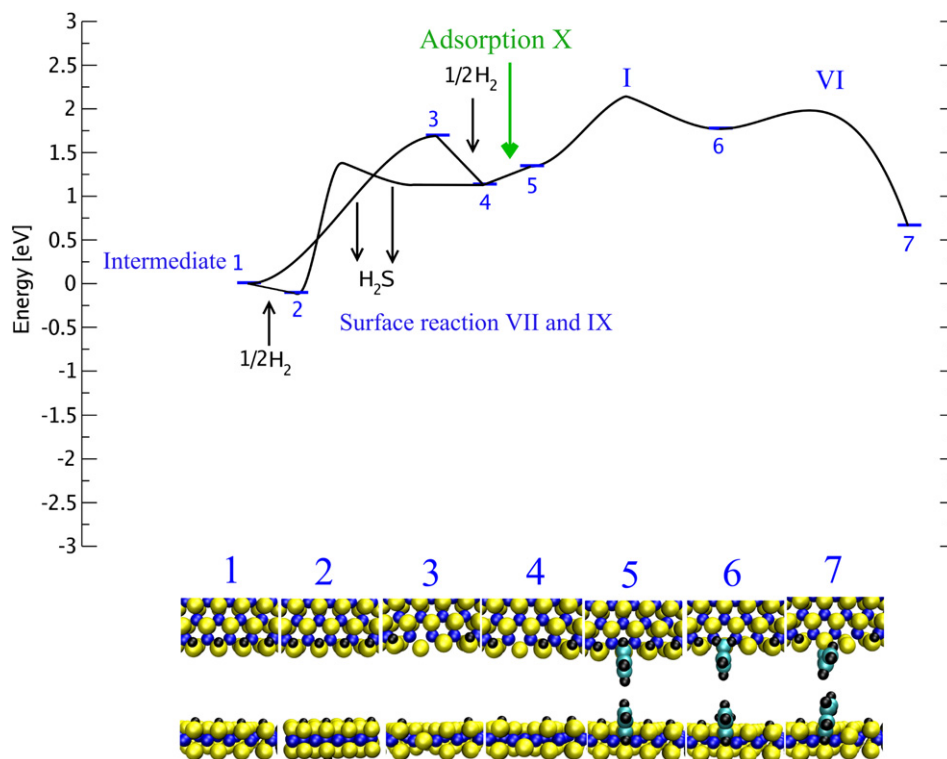


Fig. 6. The S-edge DDS pathway of thiophene. The reference energy is the equilibrium edge configuration at HDS conditions (S edge with 100% S and 100% H) and thiophene in the gas phase. The color scheme for the atoms is the same as in Fig. 1. Arabic numerals denote intermediates, and Roman numerals denote reactions. (For interpretation of the references to color in this figure legend, the reader is referred to the web version of this article.)

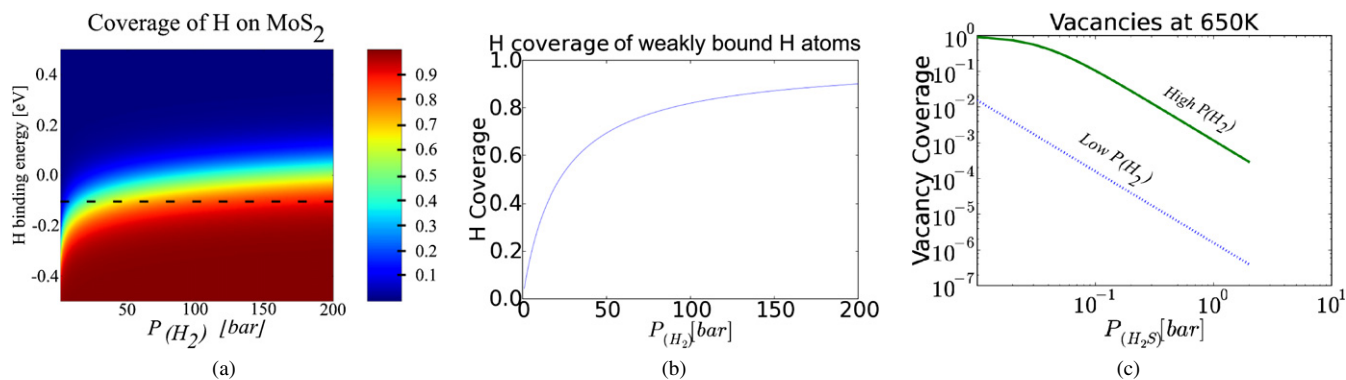


Fig. 7. H and vacancy coverages at 650 K. (a) Contour plot of the H coverage as a function of the partial pressure of hydrogen and H binding energies. The dotted line marks the binding energy of weakly bound H atoms. (b) H coverage of weakly bound H at the S edge dimers. (c) Coverage of vacancies at high and low hydrogen pressure.

ergy of -0.1 eV. Fig. 7a shows the calculated coverage of H as a function of the hydrogen pressure and H binding energy. It is seen that the strongly bound H will have 100% coverage; that is, all available sites will be filled, whereas the coverage of the weaker bound H will depend on the H_2 pressure. Fig. 7b shows the coverage of the weakly bound and thus more reactive H atoms. Many of the steps in the different HDS pathways involve H, and the barriers of these reactions likely are also lowered if the coverage of the weakly bound H is appreciable. A similar effect cannot occur at the Mo edge, because the differential H binding energy from 50 to 75% H coverage is 0.4 eV, which, according to Fig. 7a, corresponds to 0% coverage.

As discussed above, the creation of vacancies at the S edge involves reactions with H atoms, with the amount of vacancies depending on the partial pressure of hydrogen and the H coverage. Fig. 7c shows an estimate of the coverage of vacancy sites at the S edge under different reaction conditions. High H_2 pressure refers to the regime in which only the weakly bound H is involved in vacancy formation, and low H_2 pressure refers to the regime in which only strongly bound H is involved in vacancy formation. The calculations are based on the dissociative H_2S adsorption energy and assume that equilibrium is reached and that the H_2S entropy of the adsorbed state is 0 eV/K. For a particular choice of conditions like

($P_{\text{H}_2} = 10$ bar, $P_{\text{H}_2}/P_{\text{H}_2\text{S}} = 100$, and $T = 650$ K), which correspond to the low-pressure region, there is a vacancy coverage of 0.0001; however, as can be seen in Fig. 7c, this changes with reaction conditions, and the coverage of vacancy sites at the S edge typically will be in the range of 10^{-6} –0.1. This is much lower than the coverage of Mo edge brim site, which is close to 100%. The difference in availability of active sites has important catalytic consequences, and the active sites at the S edge must be far more active than the Mo edge brim site to play any role in HDS reactions.

3.6. Hydrogenation reactions

The HYD pathway is especially important for the HDS of larger molecules like DBT and is the dominating reaction pathway for the desulfurization of 4,6-DMDBT [4,7,19,27]. Although the present investigation deals with desulfurization of the much simpler and more reactive thiophene molecule, many of the hydrogenation steps observed presently likely will also be important for the key features of the hydrogenation steps of the aromatic rings in the more complex molecules. Here we analyze the relative importance of the S edge vacancy site and the Mo edge brim site in hydrogenation reactions, then examine to what extent the elementary reactions and hydrogenation reaction pathways presented in the preceding sections may describe the kinetic observations reported in the literature.

Thiophene is found to bind quite weakly (-0.1 eV) to the Mo edge brim site, but the bond is still 0.3 eV stronger than that at the S edge vacancy site. These adsorption energies will become more exothermic if van der Waals forces can be included. Moreover, the barrier for the initial hydrogenation elementary step at the Mo edge brim site is 0.2 eV lower than at the S edge vacancy site. Based on this and the higher number of active sites at the Mo edge, it is concluded that hydrogenation reactions most likely occur at the Mo edge brim site. The difference in hydrogenation activation energy between the Mo edge brim site and the S edge vacancy site is probably related to the different H binding energy at the two edges. H is bound more weakly at the Mo edge than at the S edge. The differential desorption energy of 0.5 H_2 from the equilibrium structures is 0.3 eV/(0.5 H_2) at the Mo edge, compared with 0.6 eV/(0.5 H_2) at the S edge. Thus hydrogen may be bound too strongly at the S edge, which could explain why the H transfer processes involved in hydrogenation of thiophene on the Mo edge in Fig. 3 have barriers only equal to or very close to the thermochemical differences, whereas Fig. 4 shows that there are significant barriers at the S edge.

It has been reported that hydrogenation reactions are not significantly poisoned by H_2S [27]. This has been difficult to reconcile with vacancies as the active sites, but the present finding that the hydrogenation reactions occur at the Mo brim sites without involving a vacancy explains the low inhibiting effect of H_2S on hydrogenation.

The literature reports that the HYD pathway is most important for sterically hindered molecules like 4,6-DMDBT [4,7,27]. Therefore, the hydrogenation site must be able to adsorb the sterically hindered molecules. The Mo edge brim site is

a very open site that can adsorb thiophene in both the η_1 and η_5 modes. These adsorption modes are of such a character that analogue adsorption of DBT or 4,6-DMDBT is probably not sterically hindered. However, the vacancy site at the S edge is subject to steric constraints. This further supports the aforementioned conclusion that these sites are not expected to be involved in the hydrogenation of both smaller and larger sulfur-containing molecules.

During real feed HDS, the catalysts are also exposed to high concentrations of aromatics and different types of nitrogen-containing compounds [1,2]. The present findings elucidate the inhibition mechanism of the HYD pathway, in which such heterocyclic organic compounds are found to inhibit hydrogenation. Recently, we have investigated the inhibiting effect of basic nitrogen compounds using pyridine as an example. We found that pyridine is an inhibitor [58], because it not only can adsorb like benzene to the brim site, but also is able to react with H^+ from neighboring SH groups, resulting in the formation of a pyridinium ion, which adsorbs more strongly than pyridine. The thiophene adsorption energy is -0.1 eV, significantly lower than that of the pyridinium ion (-0.6 eV) [58]. These results allow us to explain the role of pyridine as an inhibitor and to understand the different observed kinetics of feeds including basic nitrogen-containing organic compounds.

3.7. S–C bond scission reactions

We investigated S–C scission reactions belonging to either the HYD or the DDS pathway. The distinction between the HYD and the DDS pathways is that in the DDS pathway, scission of the S–C bond (reaction VI) occurs after the first hydrogenation reaction (reaction I), whereas in the HYD pathway, S–C scission occurs after further hydrogenation (reaction II) of 2-hydrothiophene into 2,5-dihydrothiophene. We investigated the S–C scission reaction for three different S–C scission reactions: in 2-hydrothiophene (leading to DDS), in 2,5-dihydrothiophene, and in *cis*-2-butenethiolate. The latter two steps are the first and second S–C scission steps involved in the HYD pathway. In Sections 3.2–3.4 we discuss how the HYD or DDS pathways can occur at either the Mo or S edge. However, the reactants and intermediates are not forced to go through all of the elementary reactions at one edge exclusively, because the intermediates may move from one site to another, either by surface diffusion or by desorption and gas-phase diffusion. The likelihood of moving from a site at one type of edge to a site at another through desorption and gas-phase diffusion depends on the relative adsorption energy of the intermediates. The green lines in Figs. 3 and 4 indicate the adsorption energies of reactants and intermediates (reactions X–XIII); the adsorption energies are also tabulated in Tables 1 and 2. We see the quite general trend that all of the intermediates adsorb at the S edge vacancy site rather than at the Mo edge; in contrast, the reactant thiophene adsorbs most strongly at the Mo edge brim site. Therefore, it is possible that some of the elementary reactions may start at the Mo edge brim, followed by desorption of intermediates and re-adsorption at the S edge, where the reaction may be completed.

Table 2
Differential adsorption energies of the intermediates in thiophene HDS

| | H coverage | 0.5 H ₂ (eV) | Thiophene (eV) | 2,5-Dihydro- thiophene (eV) | <i>Cis</i> -2-butenethiol (eV) |
|---------|----------------|----------------------------|--|--------------------------------|--------------------------------|
| S edge | 100% H, 100% S | -0.11 | | | |
| | 75% H, 87.5% S | | 0.21 | -0.59 | -0.52 |
| | 50% H, 87.5% S | -0.56 | 0.05 | -0.85 | -0.62 |
| | 25% H, 87.5% S | -0.48 | | | |
| Mo edge | 50% H, 50% S | | -0.07 ^a (-0.02) ^b | -0.12 | |
| | 25% H, 50% S | -0.33 | | -0.09 | -0.12 |

^a Perpendicular adsorption.

^b Parallel adsorption.

Later we discuss where the three different S–C reactions will occur, how reaction conditions influence the relative importance of the Mo edge brim site and the S edge vacancy site, and the interplay between these sites. The S–C scission in 2-hydrothiophene (reaction VI) is an intramolecular elimination reaction involved in DDS that does not involve a hydrogen from a neighboring –SH group as for the other S–C scission reactions investigated. The activation energy is 0.2 eV at the S edge vacancy site and 1.1 eV at the Mo edge brim site (see Table 1). The low barrier at the S edge vacancy site indicates that this site is able to break S–C bonds by elimination, whereas the high barriers at the Mo edge brim show that this site is not well suited for the elimination reaction. It should be emphasized that reaction VI occurs after the initial hydrogenation reaction (reaction I), and, as mentioned in Section 3.6, this reaction occurs primarily at the Mo edge brim. But the DDS path cannot easily continue at this edge, because reaction VI has a high barrier at the Mo edge brim site, and this reaction is competing with the further hydrogenation reaction (reaction II) involved in the HYD pathway. However, the DDS of thiophene possibly can occur if 2-hydrothiophene can move from the Mo edge to the S edge by surface diffusion. Thus, a region with high reactivity could be close to the corner region between a Mo edge and an S edge. Another possibility is that 2,5-dihydrothiophene formed at the Mo edge brim site desorbs and readsorbs at a S edge vacancy, where it is dehydrogenated to form 2-hydrothiophene before S–C scission occurs (reaction VI). In all situations, the results suggest that the S–C scission in the DDS pathway occurs at the S edge vacancy, which is consistent with the fact that the DDS pathway is strongly inhibited by H₂S [7]. The relative rate of the DDS pathway compared with the HYD pathway seems to be quite low due to the low barriers for the competing hydrogenation reaction of 2-hydrothiophene (reaction II), but a more quantitative assessment of the relative rate of the DDS and the HYD pathway requires development of a complete microkinetic model. The present results, which show that the elimination step VI has a low barrier, indicate that the S edge vacancy site also could be the active site for other types of S–C elimination reactions, such as for thiols or S–C bond scission in the DDS mechanism of DBT or 4,6-DMDBT. It also can be speculated that the S edge vacancy site may be able to eliminate both S–C bonds in 2,5-dihydrothiophene and form butadiene in a reaction mechanism similar to that found for very small clusters [60]. Furthermore, the present findings support the proposal

that an S edge vacancy site is needed to remove S from DBT and 4,6-DMDBT [56,66].

Along with the intramolecular elimination reactions involved in DDS, we also studied the hydrogenolysis reactions involved in the HYD pathway that occur when S–C bonds are broken in 2,5-dihydrothiophene and *cis*-2-butenethiolate. The S extrusion from *cis*-2-butenethiolate consists of two elementary steps: the transfer of H from an SH group to the sulfur in *cis*-2-butenethiolate (reaction IV) and the subsequent S–C scission reaction (reaction V). The H transfer step (reaction IV) turns out to be of key importance. It has a much lower barrier at the Mo edge brim site than at the S edge, which we propose to be related to the weaker binding of H atoms at the Mo edge (see Section 3.6). In contrast to the H transfer step, the S–C scission reaction has the highest barrier at the Mo edge brim site. This appears to be analogous to the situation for step VI. The final S–C scission (reaction V) likely also will occur at the Mo edge brim site, as shown in Fig. 3, even though it has a 0.1 eV higher barrier than at a S edge vacancy site. The rate of S extrusion from *cis*-2-butenethiolate at the S edge vacancy site will be determined by the H transfer step. S extrusion from *cis*-2-butenethiolate at the S edge vacancy site is competing with the backward reaction of step III, which leads to the formation of 2,5-dihydrothiophene. The barrier of 2,5-dihydrothiophene formation is similar to the barrier of H transfer (reaction IV); thus, 2,5-dihydrothiophene may be formed and subsequently desorbed and readsorbed at the Mo edge, where *cis*-2-butenethiol formation can occur. The other possibility is that *cis*-2-butenethiolate moves to the Mo edge by surface diffusion. We did not calculate the corresponding diffusion barriers, but they can be estimated by the energy required to move *cis*-2-butenethiolate from a vacancy site to a site next to the vacancy, which is 1.1 eV.

From the foregoing discussion, we can conclude that the Mo edge brim site is the primary site of *cis*-2-butenethiol formation. In view of the results shown in Fig. 7 and the discussion in Section 3.5, it can be speculated that the H transfer step and H transfer steps in general can occur more easily at the S edge vacancy site under high hydrogen partial pressure, where weakly bound H atoms are present.

Interplay between the Mo edge brim site and the S edge vacancy site is important for the desulfurization of *cis*-2-butenethiolate. For example, the final S–C scission step may

occur at the S edge vacancy even though the *cis*-2-butenethiol intermediate is formed at the Mo edge site. Such interplay between the S and Mo edges requires that *cis*-2-butenethiol move via surface diffusion or desorb from the Mo brim site. The present study found that *cis*-2-butenethiol will easily desorb due to the weak binding (-0.1 eV) at the Mo edge brim site. In this connection, it is interesting to note that thiols have been found as intermediates in the HDS of thiophene [90]. Because of their high reactivity, they are expected to be present in very small concentrations, as also has been observed experimentally [22,90].

The rate of S removal from *cis*-2-butenethiol will depend on the coverage of *cis*-2-butenethiol at the Mo edge brim site and the S edge vacancy site. At present, the coverage of *cis*-2-butenethiol cannot be calculated with high accuracy, due to the lack of thermodynamic data on gas-phase butane thiols; nonetheless, the relative coverage can be estimated. This coverage is a function of the Gibbs free energy of adsorption. Assuming that the entropy of *cis*-2-butenethiol [96] in the gas phase is similar to the entropy of *cis*-2-pentene, and using the upper limit of the entropy loss (found by assuming that all of the entropy is lost upon adsorption), $-T\Delta S_{\text{adsorb}}$ is 2.3 eV at 650 K and 1 atm. Thus, the entropy loss dominates the Gibbs free energy of adsorption, and the coverage of *cis*-2-butenethiol will be low. The large positive Gibbs free energy leads to the following simplification

$$\theta = K \cdot P / (1 + K \cdot P) \approx K \cdot P,$$

where K is the equilibrium constant ($K = \exp(-\Delta G/k_{\text{B}}T)$), P is the partial pressure of the reactant or intermediates, and θ is the coverage of the reactant or intermediates. Assuming that the entropy loss is similar at the two edges, the relative coverage is given by

$$\theta_{\text{Sedge}}/\theta_{\text{Moedge}} = \exp(-(\Delta E_{\text{Sedge}} - \Delta E_{\text{Moedge}})/(k_{\text{B}}T)),$$

where ΔE_{Sedge} is the adsorption energy at the S edge, ΔE_{Moedge} is the adsorption energy at the Mo edge, and k_{B} is the Boltzmann constant.

The adsorption energy of *cis*-2-butenethiol is most exothermic at the S edge vacancy site: between -0.5 and -0.6 eV, depending on H coverage. In contrast, it is -0.1 eV at the Mo edge brim site. Consequently, the coverage is 3 orders of magnitude larger at the S edge vacancy site. The activity for the final S–C scission is approximately 10 times higher at the S edge vacancy site than at the Mo brim site (a barrier difference of 0.12 eV). Combining this with the higher coverage of *cis*-2-butenethiol at an S edge vacancy site means that the S edge vacancy site is approximately 10^4 times more active for the HDS of *cis*-2-butenethiol than the Mo edge brim site. The same analysis for 2,5-dihydrothiophene leads to the conclusion that the S edge vacancy site is approximately 10^6 times more active in the initial S–C bond scission of 2,5-dihydrothiophene than the Mo edge brim site.

Consequently, the S edges will contribute more to the overall activity than the Mo edge if the S edge vacancy coverage is larger than approximately 10^{-4} , which (as shown in Fig. 7c) is the case at high H_2 pressure or H_2S pressure <0.1 bar. The

picture is expected to differ somewhat for species like DBT and 4,6-DMDBT, in which geometrical hindrance of adsorption plays a larger role. For these species, the difference in adsorption energy between the different sites also may be larger and this also is expected to play a role. It can be added that the relative contributions of the different MoS_2 edges also depend on the sulfiding conditions, which influence the relative abundance of the Mo and S edges [57].

The present study, which investigated the reactions at a single MoS_2 slab, represents the structures observed in many commercial catalysts quite well. The results indicate that the relative contribution of different pathways and interaction between the S edge and the Mo edge are different in stacked multislabs MoS_2 structures; for example, in such cases, only the top layer will expose readily accessible brim sites. This may be one reason why it is desirable to have mainly single slab catalysts in commercial catalysis, as well as why differences in activity depending on the degree of stacking degree has been found experimentally to be an important factor [97].

3.8. Possible rate-determining steps

The present results suggest that the regeneration of the active site is the crucial step in S removal. Regeneration of the active site at the Mo edge is comparable in energy barrier to the first S–C scission; at the S edge, the regeneration of the active site is the highest barrier involved in the HDS of thiophene. The barrier for regenerating the active site has the lowest value at the Mo edge; however, the barrier at the S edge can be lowered by high H_2 pressure, as discussed in Section 3.5. It is well known from the literature that H_2S acts as an inhibitor of S removal [7]; our results agree with this observation. The present results indicate that the S edge is inactive at low H_2 pressure and that catalytic reactions thus occur at the Mo edge. It is important to note that depending on the type of the active site, it can be either a site at which S is added to the equilibrium edge configuration or a site at which S is removed from the equilibrium edge configuration. Thus, a possible activity parameter could be the minimum energy required to either add or remove S from the equilibrium edge configuration. This insight can form the basis for refining the BEM model using S binding energy as the descriptor.

Various experimental studies have reported apparent activation energies in the ranges of 0.62–0.68 eV [98] and 0.83–1.01 eV [99]. Although a direct comparison to these apparent activation energies must await further study, the barriers found in the present study appear to compare well with the experimental values.

4. Conclusions

The present study has identified several HYD and DDS reaction pathways for thiophene HDS at both the Mo edge and the S edge, as summarized in Fig. 8. Note that as a starting point, we considered the edge configurations, which are thermodynamically most stable under realistic HDS conditions. These correspond to a Mo edge with 50% S coverage and 50% H

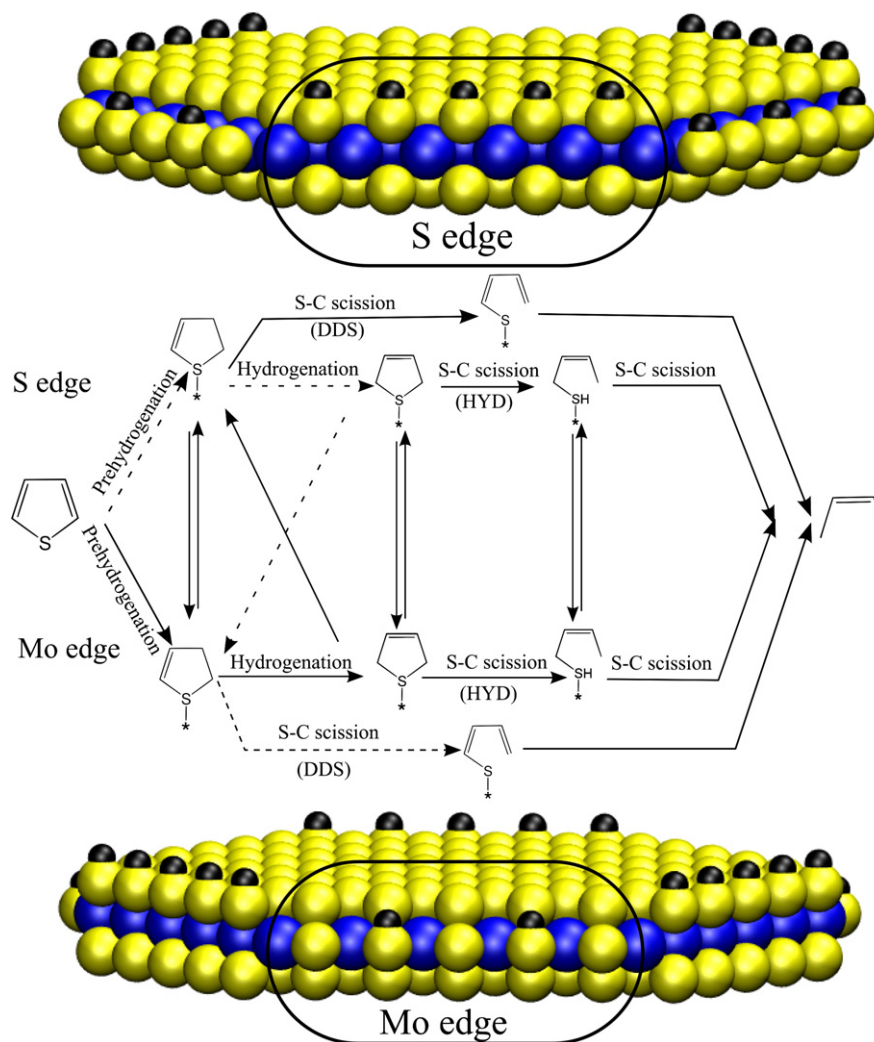


Fig. 8. Schematic overview over the reactions and MoS₂ structures involved in the HDS of thiophene. The upper part is a side view of MoS₂ perpendicular to the S($\bar{1}010$) edge, with the S and H coverage present at HDS conditions. The middle part is a schematic overview of the reactions involved in HDS of thiophene, including the possible interaction between the S($\bar{1}010$) edge and the Mo($10\bar{1}0$) edge. The dotted arrows denote reactions found to be slow. The lower part is a side view of MoS₂ perpendicular to the Mo($10\bar{1}0$) edge, with the S and H coverage present at HDS conditions.

coverage and an S edge with 100% S coverage and 100% H coverage; these structures are illustrated in Fig. 8.

Considering the elementary steps of thiophene hydrogenation and subsequent S–C bond scission, we have found some significant differences between the Mo and S edges, which can be summarized as follows:

1. H transfer and hydrogenation reactions have lower barriers at the Mo edge brim site (>0.2 eV lower than those at the S edge vacancy site).
2. Thiophene prefers to adsorb at the Mo edge brim site, where the binding is 0.3 eV stronger than at the S edge vacancy site.
3. 2,5-Dihydrothiophene and *cis*-2-butenethiol prefer to adsorb at the S edge vacancy site, where the binding is >0.4 eV stronger than at the Mo edge brim site.
4. S–C scission reactions have lower barriers at the S edge vacancy site (>0.1 eV lower than at the Mo edge brim site).

5. Regeneration of the active site has a higher barrier at the S edge (>0.5 eV higher than at the Mo edge).

Our results suggest that the HYD pathway is initiated by hydrogenation at the Mo edge, because thiophene preferentially adsorbs at the Mo edge and hydrogenation is energetically unfavorable at the S edge. In contrast, the S–C scission reaction can occur at both the Mo and S edges; which edge is preferred depends on the reaction conditions. Specifically, S–C scission preferably occurs at the Mo edge at high H₂S partial pressure and low H₂ pressures ($P_{\text{H}_2} < 80$ bar and $P_{\text{H}_2\text{S}} > 0.1$ bar), whereas the S edge is more reactive at low H₂S partial pressure or high H₂ partial pressures. This is due to the presence of different forms of adsorbed hydrogen and the resulting changes in the availability of S edge vacancy sites, which exhibit a low barrier for S–C scission.

Because the intermediates (e.g., 2,5-dihydrothiophene and *cis*-2-butenethiol) prefer to bind at the S edge rather than the Mo edge, it is possible that they diffuse to the S edge after initial

hydrogenation at the Mo edge, because desorption and diffusion are facile. Therefore, we suggest that the edges can catalyze the reaction in interplay between sites; that is, thiophene adsorbs and becomes hydrogenated at the Mo edge and subsequently diffuses to the S edge, where final S–C bond scission occurs. *Cis*-2-butenethiol is found to be an intermediate in the HYD pathway, and the low barriers of S removal from thiol at both the Mo edge brim site and the S edge vacancy site explain the high reactivity of thiols observed in kinetic and reactivity studies [7].

We find that the DDS pathway is initiated by a hydrogenation step occurring preferentially at the Mo edge, and the subsequent S–C scission occurs at the S edge. The calculated energies and barriers indicate that the DDS pathway is relatively less important than the HYD pathway for MoS₂.

The active site for thiophene HDS at the Mo edge is the so-called “brim” site, located 0.8 Å away from the edge. Note that these brim sites are present at the equilibrium edge configuration and thus should not be considered vacancies. In fact, the neighboring Mo atoms are fully coordinated by sulfur (see Fig. 8). Thus, this active site does not have to be created before the reaction can occur, but of course it must be regenerated between cycles. The active site for thiophene HDS at the S edge is a vacancy site that is not present at the equilibrium edge structure (see Fig. 8), but must be created first and subsequently regenerated between cycles. The relative concentration of S edge vacancies is significantly lower than that of the Mo edge brim sites, because the energy barrier involved in the creation of the vacancies is quite large, especially at low H₂ partial pressures. Therefore, they are present only at high H₂ partial pressures. In their absence (i.e., at low H₂ partial pressures), S–C scission must proceed by the energetically less favorable route involving the Mo edge.

Our results suggest that regeneration of the active site is a key step in the extrusion of S from thiophene at both edges. Thus, an important activity descriptor is the energy required to either add or remove S from the equilibrium edge configurations under reaction conditions.

We find that our proposed model for thiophene HDS involving the HYD and DDS pathways clarifies several experimental observations reported in the literature. We identify the Mo edge brim sites as the hydrogenation sites for the aromatic-like thiophene molecule and see that they do not require creation of a vacancy to be active. This explains the experimental observation that H₂S does not significantly inhibit hydrogenation of aromatics [7,27]. The present findings also elucidate the inhibiting effect of nitrogen-containing compounds on hydrogenation, because these species were found to preferably bind to the Mo edge brim sites [58]. At these edges, basic nitrogen containing molecules can gain extra stability through protonation by a SH group. Furthermore, the Mo edge brim site is a very “open” site that allows for adsorption of larger molecules without introducing significant steric hindrances. Thus, hydrogenation of, for example, 4,6-DMDBT likely occurs at the Mo edge brim site before desulfurization. Consequently, the S edge vacancy site also may play a large role in final removal of S from hydrogenated DBT and hydrogenated 4,6-DMDBT in a similar mechanism, where the stronger adsorption of hydrogenated in-

termediates at the S edge vacancy site aids S removal. This is consistent with the observed inhibition of these final steps by H₂S [27].

The present results show that HDS of thiophene involves a complicated interplay among edge structures, adsorption energies of reactants and intermediates, activation barriers, and reaction conditions. This may explain why researchers have found it so difficult to concur on the kinetics of thiophene HDS. It is interesting that the present results can form the basis for the development of a microkinetic model of HDS of thiophene that could be a very useful tool in quantifying the contributions of the different edges to thiophene HDS. Knowing the nature of the different sites involved in HDS can guide future design of catalysts with specific HYD/DDS properties. We can speculate that certain additives or supports may stabilize either the S or the Mo edge, and identifying such supports or additives can enable more intelligent catalyst design.

Acknowledgments

The authors thank Michael Brorson for fruitful discussions. This work was supported by the Danish Center for Scientific Computing (grant HDW-1103-06).

Supplementary information

The online version of this article contains additional supplementary information.

Please visit DOI: [10.1016/j.jcat.2007.02.028](https://doi.org/10.1016/j.jcat.2007.02.028).

References

- [1] K.G. Knudsen, B.H. Cooper, H. Topsøe, *Appl. Catal. A Gen.* 189 (1999) 205–215.
- [2] C. Song, *Catal. Today* 86 (2003) 211–263.
- [3] M.V. Landau, *Catal. Today* 36 (1997) 393–429.
- [4] B.C. Gates, H. Topsøe, *Polyhedron* 16 (1997) 3213–3217.
- [5] D.D. Whitehurst, T. Isoda, I. Mochida, *Adv. Catal.* 42 (1998) 345–471.
- [6] I.V. Babich, J.A. Moulijn, *Fuel* 82 (2003) 607–631.
- [7] H. Topsøe, B.S. Clausen, F.E. Massoth, *Hydrotreating Catalysis*, Springer-Verlag, Berlin, 1996.
- [8] R. Prins, V.H.J. De beer, G.A. Somorjai, *Catal. Rev.* 31 (1989) 1–41.
- [9] T. Kabe, A. Ishihara, W. Qian, *Catal. Surv. Jpn.* 3 (1999) 17–25.
- [10] M.L. Vrinat, *Appl. Catal.* 6 (1983) 137–158.
- [11] M.J. Girgis, B.C. Gates, *Ind. Eng. Chem. Res.* 30 (1991) 2021–2058.
- [12] T.C. Ho, *Catal. Rev.* 30 (1988) 117–160.
- [13] P.J. Owens, C.H. Amberg, *Adv. Chem. Ser.* 33 (1961) 182.
- [14] A.E. Hargreaves, J.R.H. Ross, *J. Catal.* 56 (1979) 363–376.
- [15] K.F. McCarty, G.L. Schrader, *J. Catal.* 103 (1987) 261–269.
- [16] A.N. Startsev, in: 10th Int. Congr. Catal., 1992, p. 585.
- [17] H. Schulz, D.-V. Do, *Bull. Soc. Chim. Belg.* 93 (1984) 645.
- [18] J. Leglise, J. van Gestel, J.-C. Duchet, *Adv. Hydrotreat. Catal. Prepr. Am. Chem. Soc. Div. Petrol. Chem.* 39 (1994) 533–537.
- [19] M. Houala, N.K. Nag, A.V. Sapre, D.H. Broderick, B.C. Gates, *AIChE J.* 24 (1978) 1015–1021.
- [20] K.F. McCarty, G.L. Schrader, in: 8th Int. Congr. Catal. IV, 1984.
- [21] P. Pokorný, M. Zdrážil, *Collect. Czech. Chem. Commun.* 46 (1981) 2185–2196.
- [22] H. Schulz, M. Schon, H.M. Rahman, in: L. Cervený (Ed.), *Studies in Surface Science and Catalysis*, Elsevier, Amsterdam, 2000, p. 204.
- [23] A. Borgna, E.J.M. Hensen, L. Coulier, M.H.J.M. de Croon, J.C. Schouten, J.A.R. van Veen, J.W. Niemantsverdriet, *Catal. Lett.* 90 (2003) 117–122.

- [24] M. Houalla, D.H. Broderick, V.H.J. De Beer, B.C. Gates, H. Kwart, *Am. Chem. Soc. Div. Petrol. Chem. Prepr.* 22 (1977) 941.
- [25] X.L. Ma, K. Sakanishi, I. Mochida, *Ind. Eng. Chem. Res.* 35 (1996) 2487–2494.
- [26] M. Breyse, P. Afanasiev, C. Geantet, M. Vrinat, *Catal. Today* 86 (2003) 5–16.
- [27] M. Egorova, R. Prins, *J. Catal.* 225 (2004) 417–427.
- [28] T.L. Tarbuck, K.R. McCrea, J.W. Logan, J.L. Heiser, M.E. Bussell, *J. Phys. Chem. B* 102 (1998) 7845–7857.
- [29] P. Mills, D.C. Phillips, B.P. Woodruff, R. Main, M.E. Bussell, *J. Phys. Chem. B* 104 (2000) 3237–3249.
- [30] P.C.H. Mitchell, D.A. Green, E. Payen, J. Tomkinson, S.F. Parker, *Phys. Chem. Chem. Phys.* 1 (1999) 3357–3363.
- [31] S.J. Tauster, T.A. Pecoraro, R.R. Chianelli, *J. Catal.* 63 (1980) 515–519.
- [32] H. Topsøe, R. Candia, N.-Y. Topsøe, B.S. Clausen, *Bull. Soc. Chim. Belg.* 93 (1984) 783–806.
- [33] M. Salmeron, G.A. Somorjai, A. Wold, R. Chianelli, K.S. Liang, *Chem. Phys. Lett.* 90 (1982) 105–107.
- [34] R.J.H. Voorhoeve, *J. Catal.* 23 (1971) 236.
- [35] R.J.H. Voorhoeve, J.C.M. Stuijver, *J. Catal.* 23 (1971) 243.
- [36] N.-Y. Topsøe, H. Topsøe, *J. Catal.* 139 (1993) 641–651.
- [37] B. Scheffer, N.J.J. Dekker, P.J. Mangnus, J.A. Moulijn, *J. Catal.* 121 (1990) 31–46.
- [38] D.G. Kalthod, S.W. Weller, *J. Catal.* 98 (1986) 572–576.
- [39] J.K. Nørskov, B.S. Clausen, H. Topsøe, *Catal. Lett.* 13 (1992) 1–8.
- [40] P. Zeuthen, P. Stolze, U.B. Pedersen, *Bull. Soc. Chim. Belg.* 96 (1987) 985–995.
- [41] F. Bataille, J.L. Lemberon, P. Michaud, G. Perot, M. Vrinat, M. Lemaire, E. Schulz, M. Breyse, S. Kaztelan, *J. Catal.* 191 (2000) 409–422.
- [42] F. van Looij, P. van de Laan, W.H.J. Stork, D.J. DiCamillo, J. Swain, *Appl. Catal. A Gen.* 170 (1998) 1–12.
- [43] M. Nagai, T. Kabe, *J. Catal.* 81 (1983) 440–449.
- [44] M. Nagai, T. Sato, A. Aiba, *J. Catal.* 97 (1986) 52–58.
- [45] V. LaVopa, C.N. Satterfield, *J. Catal.* 110 (1988) 375–387.
- [46] P. Zeuthen, K.G. Knudsen, D.D. Whitehurst, *Catal. Today* 65 (2001) 307–314.
- [47] P. Wiwel, K. Knudsen, P. Zeuthen, D. Whitehurst, *Ind. Eng. Chem. Res.* 39 (2000) 533–540.
- [48] M. Egorova, R. Prins, *J. Catal.* 221 (2004) 11–19.
- [49] M. Egorova, R. Prins, *J. Catal.* 224 (2004) 278–287.
- [50] T.C. Ho, *J. Catal.* 219 (2003) 442–451.
- [51] U.T. Turaga, X. Ma, C. Song, *Catal. Today* 86 (2003) 265–275.
- [52] E. Furimsky, F.E. Massoth, *Catal. Today* 52 (1999) 381–495.
- [53] C. Song, X. Ma, *Appl. Catal. B Environ.* 41 (2003) 207–238.
- [54] H. Schweiger, P. Raybaud, H. Toulhoat, *J. Catal.* 212 (2002) 33–38.
- [55] L.S. Byskov, J.K. Nørskov, B.S. Clausen, H. Topsøe, *J. Catal.* 187 (1999) 109–122.
- [56] M.V. Bollinger, K.W. Jacobsen, J.K. Nørskov, *Phys. Rev. B* 67 (2003) 085410.
- [57] J.V. Lauritsen, M.V. Bollinger, E. Lægsgaard, K.W. Jacobsen, J.K. Nørskov, B.S. Clausen, H. Topsøe, F. Besenbacher, *J. Catal.* 221 (2004) 510–522.
- [58] Á. Logadóttir, P.G. Moses, B. Hinnemann, N.-Y. Topsøe, K.G. Knudsen, H. Topsøe, J.K. Nørskov, *Catal. Today* 111 (2006) 44–51.
- [59] T. Todorova, R. Prins, T. Weber, *J. Catal.* 236 (2005) 190.
- [60] X. Yao, Y. Li, H. Jiao, *J. Mol. Struct. Theochem.* 726 (2005) 81.
- [61] J.V. Lauritsen, M. Nyberg, J.K. Nørskov, B.S. Clausen, H. Topsøe, E. Lægsgaard, F. Besenbacher, *J. Catal.* 224 (2004) 94–106.
- [62] P. Raybaud, J. Hafner, G. Kresse, H. Toulhoat, *Stud. Surf. Sci. Catal.* 127 (1999) 309–317.
- [63] S. Cristol, J.F. Paul, E. Payen, D. Bougeard, S. Clémendot, F. Hutschka, *J. Phys. Chem. B* 106 (2002) 5659–5667.
- [64] P. Raybaud, J. Hafner, G. Kresse, H. Toulhoat, *Phys. Rev. Lett.* 80 (1998) 1481–1484.
- [65] M. Neurock, R.A. van Santen, *J. Am. Chem. Soc.* 116 (1994) 4427–4439.
- [66] S. Cristol, J.F. Paul, E. Payen, D. Bougeard, F. Hutschka, S. Clémendot, *J. Catal.* 224 (2004) 138–147.
- [67] J.F. Paul, E. Payen, *J. Phys. Chem. B* 107 (2003) 4057–4064.
- [68] L.S. Byskov, M. Bollinger, J.K. Nørskov, B.S. Clausen, H. Topsøe, *J. Mol. Catal. A Chem.* 163 (2000) 117–122.
- [69] S. Cristol, J.F. Paul, E. Payen, D. Bougeard, S. Clémendot, F. Hutschka, *J. Phys. Chem. B* 104 (2000) 11220–11229.
- [70] P. Raybaud, J. Hafner, G. Kresse, S. Kasztelan, H. Toulhoat, *J. Catal.* 190 (2000) 128–143.
- [71] L.S. Byskov, B. Hammer, J.K. Nørskov, B.S. Clausen, H. Topsøe, *Catal. Lett.* 47 (1997) 177–182.
- [72] M. Sun, A.E. Nelson, J. Adjaye, *J. Catal.* 233 (2005) 411–421.
- [73] S. Helveg, J.V. Lauritsen, E. Lægsgaard, I. Stensgaard, J.K. Nørskov, B.S. Clausen, H. Topsøe, F. Besenbacher, *Phys. Rev. Lett.* 84 (2000) 951–954.
- [74] J.V. Lauritsen, S. Helveg, E. Lægsgaard, I. Stensgaard, B.S. Clausen, H. Topsøe, F. Besenbacher, *J. Catal.* 197 (2001) 1–5.
- [75] M.V. Bollinger, J.V. Lauritsen, K.W. Jacobsen, J.K. Nørskov, S. Helveg, F. Besenbacher, *Phys. Rev. Lett.* 87 (2001) 196801–196803.
- [76] A. Carlsson, M. Brorson, H. Topsøe, *J. Catal.* 227 (2004) 530–536.
- [77] B. Hinnemann, P.G. Moses, J. Bonde, K.P. Jørgensen, J.H. Nielsen, S. Horch, I. Chorkendorff, J.K. Nørskov, *J. Am. Chem. Soc.* 127 (2005) 5308–5309.
- [78] B. Hinnemann, J.K. Nørskov, H. Topsøe, *J. Phys. Chem. B* 109 (2005) 2245–2253.
- [79] S.R. Bahn, K.W. Jacobsen, *Comput. Sci. Eng.* 4 (2002) 56–66.
- [80] B. Hammer, L.B. Hansen, J.K. Nørskov, *Phys. Rev. B* 59 (1999) 7413.
- [81] H.J. Monkhorst, J.D. Pack, *Phys. Rev. B* 13 (1976) 5188–5192.
- [82] T. Böker, R. Severin, A. Müller, C. Janowitz, R. Manzke, D. Voss, P. Krüger, A. Mazur, J. Pollmann, *Phys. Rev. B* 64 (2001) 235305-1–235305-11.
- [83] K. Laasonen, A. Pasquarello, R. Car, C. Lee, D. Vanderbilt, *Phys. Rev. B* 47 (1993) 10142–10153.
- [84] N. Troullier, J.L. Martins, *Phys. Rev. B* 43 (1991) 1993–2006.
- [85] D. Vanderbilt, *Phys. Rev. B* 41 (1990) 7892–7895.
- [86] J.P. Perdew, J.A. Chevary, S.H. Vosko, K.A. Jackson, M.R. Pederson, D.J. Singh, C. Fiolhais, *Phys. Rev. B* 46 (1992) 6671.
- [87] H. Jonsson, G. Mills, K.W. Jacobsen, in: B.J. Berne, G. Cicotti, D.F. Coker (Eds.), *Classical and Quantum Dynamics in Condensed Phase Systems*, Enrico Fermi Summer School, vol. 97, World Scientific, Singapore, 1997.
- [88] S.A. Andreiev, Y. Brumer, D.R. Reichman, E. Kaxiras, P. Maragakis, *J. Chem. Phys.* 117 (2002) 4651–4658.
- [89] W. Humphrey, A. Dalke, K. Schulten, *J. Mol. Graph.* 14 (1996) 33–38.
- [90] D.L. Sullivan, J.G. Ekerdt, *J. Catal.* 178 (1998) 226–233.
- [91] A. Borgna, E.J.M. Hensen, J.A.R. van Veen, J.W. Niemantsverdriet, *J. Catal.* 221 (2004) 541–548.
- [92] A. Travert, H. Nakamura, R.A. van Santen, J.F. Paul, E. Payen, *J. Am. Chem. Soc.* 124 (2002) 7084–7095.
- [93] P. Mills, S. Koralann, M.E. Bussell, M.A. Reynolds, M.V. Ovchinnikov, R.J. Angelici, C. Stinner, T. Weber, R. Prins, *J. Phys. Chem. A* 105 (2001) 4418–4429.
- [94] R.J. Angelici, *Polyhedron* 16 (1997) 3073–3088.
- [95] S. Cristol, J. Paul, C. Schovsbo, E. Veilly, E. Payen, *J. Catal.* 239 (2006) 145–153.
- [96] D.R. Lide, *CRC Handbook of Chemistry and Physics*, 83rd ed., CRC Press, Boca Raton, 2002.
- [97] M. Daage, R.R. Chianelli, *J. Catal.* 149 (1994) 414–427.
- [98] E.J.M. Hensen, H.J.A. Brans, G.M.H.J. Lardinois, V.H.J. de Beer, J.A.R. van Veen, R.A. van Santen, *J. Catal.* 192 (2000) 98–107.
- [99] M.J. Ledoux, O. Michaux, G. Agostini, P. Panissod, *J. Catal.* 102 (1986) 275–288.